Hierarchical multi-population viability analysis

Douglas R. Leasure,[1,6] Seth J. Wenger,[1] Nathan D. Chelgren,[2] Helen M. Neville,[3] Daniel C. Dauwalter,[3] Robin Bjork,[3] Kurt A. Fesenmyer,[3] Jason B. Dunham,[2] Mary M. Peacock,[4] Charlie H. Luce,[5] Abby C. Lute,[5] and Daniel J. Isaak[5]

[1]*University of Georgia, 203 D.W. Brooks Drive, Athens, Georgia 30602 USA*
[2]*U.S. Geological Survey, Forest and Rangeland Ecosystem Science Center, 3200 SW Jefferson Way, Corvallis, Oregon 97331 USA*
[3]*Trout Unlimited, 910 West Main Street no 342, Boise, Idaho 83702 USA*
[4]*Department of Biology, University of Nevada—Reno, Reno, Nevada 89557 USA*
[5]*US Forest Service, 322 E Front St, Boise, Idaho 83702 USA*

Abstract. Population viability analysis (PVA) uses concepts from theoretical ecology to provide a powerful tool for quantitative estimates of population dynamics and extinction risks. However, conventional statistical PVA requires long-term data from every population of interest, whereas many species of concern exist in multiple isolated populations that are only monitored occasionally. We present a hierarchical multi-population viability analysis model that increases inference power from sparse data by sharing information among populations to assess extinction risks while accounting for incomplete detection and sampling biases with explicit observation and sampling sub-models. We present a case study in which we customized this model for historical population monitoring data (1985–2015) from federally threatened Lahontan cutthroat trout populations in the Great Basin, USA. Data were counts of fish captured during backpack electrofishing surveys from locations associated with 155 isolated populations. Some surveys (25%) included multi-pass removal sampling, which provided valuable information about capture efficiency. GIS and remote sensing were used to estimate August stream temperatures, peak flows, and riparian vegetation condition in each population each year. Field data were used to derive an annual index of nonnative trout densities. Results indicated that population growth rates were higher in colder streams and that nonnative trout reduced carrying capacities of native trout. Extinction risks increased with more environmental stochasticity and were also related to population extent, water temperatures, and nonnative densities. We developed a graphical user interface to interact with the fitted model results and to simulate future habitat scenarios and management actions to assess their influence on extinction risks in each population. Hierarchical multi-population viability analysis bridges the gap between site-level field observations and population-level processes, making effective use of existing datasets to support management decisions with robust estimates of population dynamics, extinction risks, and uncertainties.

Key words: conservation; extinction risk; hierarchical Bayesian time series; imperfect detection; isolated populations; Lahontan cutthroat trout; observation model; population viability analysis; removal sampling; Ricker model.

INTRODUCTION

Population viability analysis (PVA) plays a central role at the crossroads of population ecology, conservation biology, and environmental policy (Beissinger and McCullough 2002, Morris and Doak 2002). It bridges the gap between theoretical and applied ecology, and it is sought after to forecast dynamics of imperiled populations and to estimate extinction risks under different management or climate scenarios. Applications have included high profile conservation efforts for threatened species including grizzly bears (Shaffer 1978, 1983) and northern spotted owls (Lande 1988, Doak 1989, Boyce 1994). However, traditional demographic PVA requires many years of data from each population to be assessed. Monitoring programs for imperiled species generally collect data from multiple populations, but may not monitor any single population enough to perform a data-driven PVA. A statistical framework is needed that can harness

sparse data that already exist from across the range of a species to rigorously assess population viability for all of its isolated populations. This requires a synthesis of classical concepts in theoretical ecology (May 1973, Gotelli 2008) and conservation biology (Beissinger and McCullough 2002, Morris and Doak 2002) with recent advances in occupancy modeling (Royle and Dorazio 2008) and Bayesian statistics (Gelman et al. 2013, Hobbs and Hooten 2015).

Two paradigms in conservation biology have developed in parallel (Caughley 1994): The declining population paradigm and the small population paradigm. The declining population paradigm focuses on environmental or demographic factors associated with population declines, often with the intention of manipulating those factors (Boyce 1992, Akcakaya and Raphael 1998). Favored by managers for its practicality, this approach often relies on site-level observations of abundance and habitat. The challenge with this approach can be extrapolating inferences to population-level processes like recruitment, demographic stochasticity, and extinction. The small population paradigm is more focused on population-level processes, relying heavily on concepts from theoretical ecology. The primary goal is to identify minimum viable population sizes (Shaffer 1981) that

[6] E-mail: doug.leasure@gmail.com

can persist in the face of demographic and environmental stochasticity (May 1973), without regard for habitat factors associated with population dynamics. A challenge with this approach is incorporating site-level observations to inform parameter estimates rather than relying on expert opinion or pure simulation studies. PVA models that include demographic and environmental stochasticity while also estimating effects of habitat covariates can be used to explore the intersection of these two paradigms theoretically and to better harness the strengths of both approaches for applied conservation issues.

The challenge of linking site-level observations to population-level processes has been a wedge between the declining- and small-population paradigms, and more generally, between applied and theoretical ecology. Population-level processes are often difficult to observe directly because they operate at larger spatial and temporal scales than field sampling can accommodate. There are several challenges: (1) accurately estimating site abundances using field observations that imperfectly detect organisms, (2) scaling-up site abundances to estimate total population sizes while accounting for sampling error and unsampled habitat, and (3) obtaining sufficient time-series data to estimate demographic rates and their responses to the environment. There has been significant progress in each of these areas using hierarchical observation and process models (Berliner 1996, Royle and Dorazio 2008) and integrated population models (Shaub and Abadi 2011).

Imperfect detection is a topic rich with theoretical advancements followed by widespread conservation applications (MacKenzie et al. 2006, Royle and Dorazio 2008). Methods have historically focused on site-level abundances and covariate effects rather than population-level processes, but recent progress has linked these models to time-series models and demographic processes at the scale of the sample site. N–mixture models (Royle 2004) have been particularly influential because they require only count data, avoiding resource intensive mark–recapture surveys. We will use the term N–mixture models to include the class of models designed for counts of unmarked individuals, be it repeated point counts common for birds or removal sampling common for fish. Appropriate count data are collected by many conservation monitoring programs and historical data are available for many species. N–mixture models glean information from repeated counts of unmarked animals at each site to estimate true site abundances, with the critical assumption that the site is closed to migration and there are no births or deaths during the survey period. Dail and Madsen (2010) relaxed these assumptions by explicitly modeling "gains" (births + immigration) and "losses" (deaths + emigration) to the population each year. Zipkin et al. (2014) added stage structure to this framework, and Kanno et al. (2015) added density-dependent recruitment and covariate effects. Kanno et al. (2015) assumed that covariate effects on demographic rates were consistent among sites, allowing them to leverage data from multiple sites to estimate these effects, which may have otherwise required many years of data from each site. These models account for imperfect detection and they link site-level observations to demographic processes, but they assume that a sampled site is representative of the entire population and independent from other sampling locations. For this reason, they cannot incorporate data from multiple sample sites within a population, and most importantly, they cannot estimate total population sizes or extinction risks.

Incomplete sampling from the total spatial extent of a population is a necessary limitation for almost all monitoring programs, but sampling error can bias estimates of population size and extinction risk with a tendency toward overly pessimistic estimates of viability (Staples et al. 2004). Carlin et al. (1992) and Berliner (1996) provided a hierarchical Bayesian framework for time series models (i.e., state-space models) that explicitly accounts for both the observation process (i.e., field surveys) and its relationship to unobserved demographic processes. Clark (2007) thoroughly explored a range of ecological applications for this class of models, including concepts like age structure, density dependence, demographic and environmental stochasticity, mark–recapture studies, and covariate effects. Hobbs and Hooten (2015) added a sampling model to this hierarchical structure (i.e., process, sampling, and observation model) to accommodate data arising from incomplete sampling of a population's spatial extent. The sampling model also allowed them to include multiple sampling locations from a single population. This is a critical step towards leveraging existing data from population monitoring programs to assess population viability because it allows inferences to be made for the total population extent rather than being limited to the sampling location. This is necessary to estimate total population sizes and overall extinction risks. Unfortunately, there are few cases where sufficient time series data exist from a single population to fit these models.

We developed a hierarchical Bayesian model for population viability analysis that uses data from multiple isolated populations simultaneously to bolster inference power across the range of a species and into the future. Hierarchical multi-population viability analysis (MPVA) bridges the gap between the declining- and small-population paradigms by including demographic and environmental stochasticity while also relating demographic rates to environmental covariates. Wenger et al. (2017) previously introduced the process model that lies at the core of MPVA, demonstrating how information can be borrowed from well-sampled populations to predict viability of data-poor populations. However, they did not link this to an observation model or sampling model, which is necessary to derive the full benefits of the approach. Here we present the full hierarchical model, which can accommodate counts of unmarked individuals from multiple sampling locations within each population, making it appropriate for use with many existing datasets. The Bayesian framework provides flexibility to customize the model for specific datasets and it explicitly accounts for uncertainty at each level of the model. Hierarchical MPVA makes it possible to: (1) Use all available abundance data from multiple isolated populations, (2) Account for observation and sampling error, (3) Infer population-level parameters from site-level observations, (4) Estimate effects of spatio-temporal covariates on demographic rates, and (5) Account for demographic and environmental stochasticity.

We provide an overview of a general model structure for hierarchical MPVA along with a case study using 30 years of sporadic population monitoring data from 155 isolated

populations of federally threatened Lahontan cutthroat trout (*Oncorhynchus clarkii henshawi*).

OVERVIEW: MULTI-POPULATION VIABILITY ANALYSIS

Following the structure outlined by Hobbs and Hooten (2015), a hierarchical MPVA model has three components: an observation model, a sampling model, and a process model. The observation model accounts for imperfect detection of organisms during field surveys at each site. The sampling model accounts for sampling error that arises from incomplete sampling from the spatial extent of a population and non-uniform distributions of individuals. The process model represents the temporal dynamics of population growth and can include features like density dependence, age structure, and environmental stochasticity.

Biological data for MPVA should include multiple populations monitored over multiple years, with multipass surveys conducted at some sites. Time series may include years without data. Observations $y_{i,t,j,m}$ are counts of individuals observed during each survey pass m at site j in year t for population i. Surveys could be repeated point counts, removal sampling, multi-surveyor designs, distance sampling, or virtually any other count-based survey design for which an appropriate observation model can be specified. Age or stage structure may be included or not.

Hierarchical MPVA has three key model parameters: (1) Demographic rates $R_{i,t}$ from the process model: rates of population change from year-to-year, (2) Occurrence probabilities $\upsilon_{i,t,j}$ from the sampling model: probability that an individual from the population would occur at sample site j and Detection probabilities $p_{i,t,j,m}$ from the observation model: probability that an individual occupying a site would be observed during survey m.

A general model structure for hierarchical MPVA can be written as

$$[N_{i,t}|N_{i,t-1}, R_{i,t}]$$
$$[R_{i,t}|x_{i,t}, \boldsymbol{\beta}]$$
$$[n_{i,t,j}|\upsilon_{i,t,j}, N_{i,t}]$$
$$[y_{i,t,j,m}|p_{i,t,j,m}, n_{i,t,j}].$$

Bracket notations represent generic probability distributions (i.e., the first line indicates that $N_{i,t}$ is stochastic and dependent on $N_{i,t-1}$ and $R_{i,t}$). $N_{i,t}$ are total population sizes each year, $n_{i,t,j}$ are total abundances at each site j, and $y_{i,t,j,m}$ are counts of individuals observed during each survey m. The $x_{i,t}$ are spatio-temporal covariates and $\boldsymbol{\beta}$ are their effects on population growth rates $R_{i,t}$.

Modeling $R_{i,t}$ as a function of spatiotemporal covariates enables data-driven population simulations anywhere within the modeling domain where covariates can be measured or estimated. Remotely sensed and GIS-based covariates are valuable in this context because they provide consistent range-wide habitat measurements annually. This general structure for hierarchical MPVA can be customized by selecting appropriate error structures, functional relationships, and covariates for each sub-model based on characteristics of the data and expectations about how the system behaves.

CASE STUDY: LAHONTAN CUTTHROAT TROUT

We demonstrate MPVA using data from multiple monitoring programs for federally threatened Lahontan cutthroat trout (LCT; *Oncorhynchus clarkii henshawi*) throughout its range in Nevada, Oregon, and California, USA. We chose this species because it exists in isolated populations, there is a substantial amount of data available, and it is a focus of management programs. Our intention was to demonstrate MPVA using a real-world example to highlight key concepts and model results, but it is beyond the scope of this paper to give thorough treatment to ecological inferences and management recommendations. Our LCT model was developed in collaboration with project partners who contributed data and expert opinion. These included representatives from U.S. Fish and Wildlife Service, Bureau of Land Management, U.S. Forest Service, Nevada Department of Wildlife, Oregon Department of Fish and Wildlife, and California Department of Fish and Wildlife.

We aggregated LCT survey data from project partners to build a database that included 155 populations with data from the 30-yr period from 1984 to 2015. This included 71 streams where LCT were extirpated. Traditional population viability analyses were previously conducted for 13 populations individually (Peacock and Dochtermann 2012) providing 5–10 consecutive years of data for these populations from 1993 to 2002. The rest of the data were from sporadic sampling events with few consecutive years of data for most populations. Spatial coverage of sampling was usually small compared to populations' spatial extents (mean = 3%, maximum = 20%). Multi-pass removal sampling (i.e., repeated sampling without replacement from a closed habitat unit) was conducted during 25% of sampling events, and single-pass sampling was conducted during the rest. Our goals for the Lahontan Cutthroat Trout MPVA model were: (1) Estimate population sizes and extinction probabilities for populations with monitoring data, (2) Assess population viability for unsampled streams using environmental covariates only, and (3) Evaluate potential effects of management actions and future environments on population viability.

MPVA model development

Throughout the paper, we numbered only the mathematical expressions that were used in multi-population viability analysis for Lahontan cutthroat trout. Unnumbered mathematical expressions were included to demonstrate connections with previously published models and possible model extensions. The directed acyclic graph (Fig. 1) provides an overview of how parameters and data throughout the model relate to one another and to numbered expressions in the text. Table 1 provides definitions for symbols.

Process model.—The process model represents population change from one year to the next. From classical population ecology, there are a number of models for density-dependent population growth that may be appropriate to use with count data (Verhulst 1838, Beverton and Holt 1957). If age or stage structured counts are available, structured population dynamics could potentially be modeled (Leslie 1945). We will focus on a basic Ricker model (Ricker 1954), which
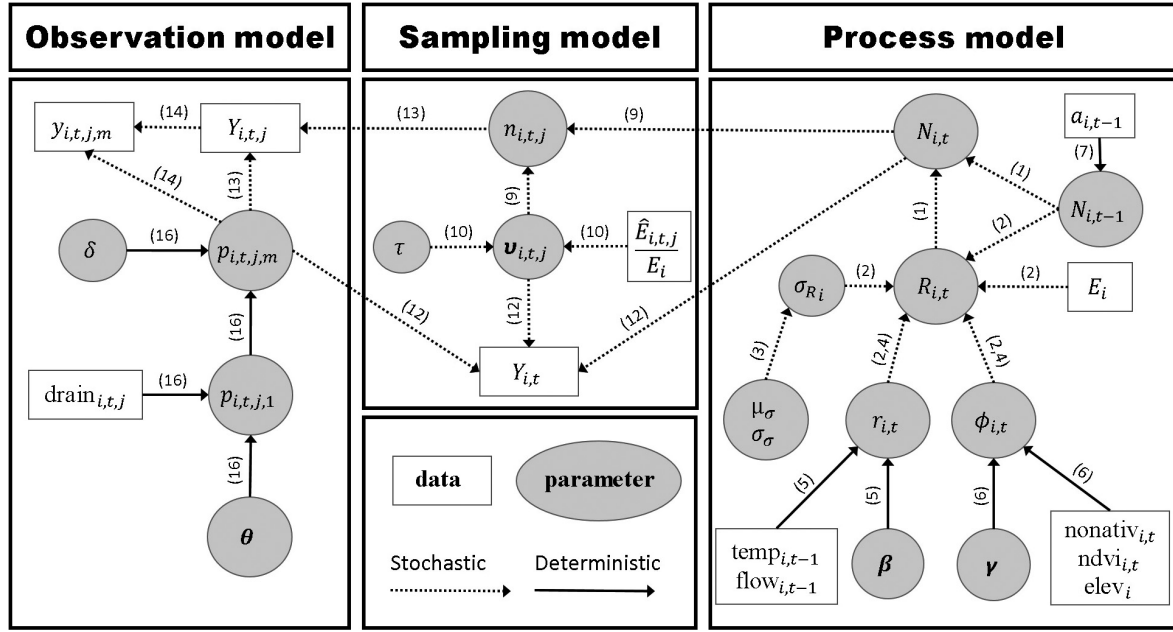
Fig. 1. Directed acyclic graph (DAG) for hierarchical multi-population viability analysis. Numbers refer to mathematical expressions in the text that are represented by each arrow. Symbols are defined in Table 1.

is fundamental to theoretical ecology and has been widely applied for management. This model assumes density-dependent population growth with no age structure. It is often written in the form

$$N_t = N_{t-1} e^{r(1-\frac{N_{t-1}}{K})}$$

where N_t is population size (age 1 +) in year t, r is the intrinsic rate of population growth, and K is carrying capacity. This is an exponential growth model with growth rates that decline toward zero as the population approaches carrying capacity.

One of the primary goals for MPVA is to model multiple populations simultaneously to reduce data requirements from any single population by sharing information among populations. To make carrying capacities K_i comparable among populations occupying different spatial extents E_i, we redefined them in terms of density rather than abundance

$$N_{i,t} = N_{i,t-1} e^{r(1-\frac{N_{i,t-1}/E_i}{K_i})}.$$

Attempting to estimate both free parameters r and K_i can lead to identifiability issues (multiple parameter states that produce identical model behavior) because their relationship is multiplicative in this model. To improve identifiability, we used an alternative formulation of the Ricker model (Hobbs and Hooten 2015)

$$N_{i,t} = N_{i,t-1} e^{r+\phi_i \frac{N_{i,t-1}}{E_i}}.$$

This is simply an algebraic rearrangement where $\phi_i = (-r/K_i)$, representing the effect of density dependence. The

units for ϕ_i are changes in realized growth rates resulting from adding one individual per unit area to last year's population. This linear formulation improves our ability to model r and ϕ as a function of spatio-temporal covariates $x_{i,t}$

$$r_{i,t} = \beta_0 + \beta_1 x_{i,t} +$$
$$\phi_{i,t} = \gamma_0 + \gamma_1 x_{i,t} + \;.$$

So far, this deterministic process model is a multi-population form of a simple exponential growth model with growth rates that are a linear function of covariates, density, and their interactions. It could be re-written as:

$$N_{i,t} = N_{i,t-1} e^{\beta_0+\beta_1 x_{i,t}+\gamma_0 \frac{N_{i,t-1}}{E_i}+\gamma_1 x_{i,t} \frac{N_{i,t-1}}{E_i}+}$$

At this stage of formulation, the model does not account for demographic and environmental stochasticity. Random variation is critical to account for because it can drive small populations extinct (Shaffer 1981). Demographic stochasticity arises from the fact that reproduction and survival are integer-based processes (May 1973). If average per-capita recruitment is 2.5, most adults produce either two or three offspring but never 2.5 offspring. This can cause population sizes to drift randomly over time. To capture this, we modeled population sizes $N_{i,t}$ as a Poisson process

$$N_{i,t} \sim \text{Poisson}\left(N_{i,t-1} e^{R_{i,t}}\right) \qquad (1)$$

where $R_{i,t}$ are realized population growth rates.

Environmental stochasticity (May 1973) arises from variation in unmodeled environmental factors that affect demographic rates. Following others, we modeled this as normally distributed random variation in realized population growth

TABLE 1. Definitions of symbols with references to expressions where they are used.

Symbol	Definition	Expression
Data		
$y_{i,t,j,m}$	Count of individuals observed each survey pass	15
$Y_{i,t,j}$	Total observed individuals among passes at a site	14
$Y_{i,t}$	Total observed individuals among all sites	13
$a_{i,t}$	Translocated individuals	8
E_i	Extent of population (length or area)	5
$\tilde{E}_{i,t,j}$	Extent of sample site (length or area)	11
$\text{temp}_{i,t}$	Water temperature	6
$\text{flow}_{i,t}$	Peak flow	7
$\text{nonativ}_{i,t}$	Density of nonnative trout	7
$\text{ndvi}_{i,t}$	Riparian vegetation condition	7
elev_i	Binary elevation indicator (above or below 2,000 m)	7
Parameters		
$N_{i,t}$	Population size	2,8,5,8,2,13
λ_i	Expected initial population size	8
$R_{i,t}$	Realized population growth rate	2,3,5
$r_{i,t}$	Intrinsic population growth rate	5,6
$\boldsymbol{\beta}$	Effects of covariates on $r_{i,t}$	6
$\varphi_{i,t}$	Strength of density dependence	5,7
$\boldsymbol{\gamma}$	Effects of covariates on $\varphi_{i,t}$	7
σ_{Ri}	Environmental stochasticity	3,3
μ_σ	Mean of σ_{Ri} among populations	3
σ_σ	Standard deviation of σ_{Ri} among populations	3
$n_{i,t,j}$	Site abundance	2,14
$v_{i,t,j}$	Occupancy probability	2,11,13
τ	Sampling precision	11,12
$p_{i,t,j,m}$	Detection probability during pass m	13,14,15,16,17
$Q_{i,t,j,m}$	Probability of non-detection in prior passes	15,16
δ	Decline in detection rates in each subsequent pass	15,18
$\boldsymbol{\theta}$	Effects of covariates on first-pass detection rates	15,18

rates (Morris and Doak 2002, Clark and Bjornstad 2004, Gotelli 2008)

$$R_{i,t} \sim \text{Normal}(\bar{R}_{i,t}, \sigma_{Ri}) \qquad (2)$$

where $\bar{R}_{i,t}$ is the mean and σ_{Ri} is the standard deviation. σ_{Ri} is a population-specific estimate of environmental stochasticity, and it can be modeled hierarchically with hyper-parameters shared among all populations

$$\sigma_{Ri} \sim \text{Half Cauchy}(\mu_\sigma, \sigma_\sigma)$$
$$\mu_\sigma, \sigma_\sigma \sim \text{Uniform}(0, 10). \qquad (3)$$

We used Half-Cauchy distributions to represent standard deviations in realized growth rates following recommendations of Gelman (2006) for hierarchical variance models. The hierarchical structure shares information among populations to estimate this data-hungry parameter, and it constrains estimates of environmental stochasticity to be similar among populations unless observed data provide significant

evidence to the contrary. It also allows predictions for populations where no data have been collected. Uniform hyper-priors were selected to be uninformative. As a practical decision to improve convergence, we truncated the distribution of σ_{Ri} to be above 0.01, avoiding unrealistic accumulation of density near zero that sometimes occurred. For this parameter to approach zero would imply that our four covariates explained *all* of the variation in realized growth rates, which is extremely unlikely.

In this stochastic Ricker model, expected realized population growth rates $\bar{R}_{i,t}$ are a linear function of the prior year's population density

$$\bar{R}_{i,t} = r_{i,t} + \phi_{i,t}\frac{N_{i,t-1}}{E_i} \qquad (4)$$

where the intercept $r_{i,t}$ is intrinsic population growth rate and the slope $\phi_{i,t}$ is the effect of density dependence. We selected spatio-temporal covariates as predictors of $r_{i,t}$ and $\phi_{i,t}$ in collaboration with project partners. We emphasized remotely sensed and GIS-based covariates because they can be measured consistently every year for all populations. We included two predictors of intrinsic population growth rates

$$r_{i,t} = \beta_0 + \beta_1 \text{temp}_{i,t-1} + \beta_2 \text{flow}_{i,t-1}$$
$$\boldsymbol{\beta} \sim \text{Normal}(0, 10). \qquad (5)$$

The normal priors for elements in the vector of regression coefficients $\boldsymbol{\beta}$ were selected to be uninformative.

The variable $\text{temp}_{i,t-1}$ is mean August stream temperature estimated using a regional stream temperature model (Isaak et al. 2017) averaged throughout each population's extent each year. We expected intrinsic population growth rates to increase with colder stream temperatures because the trout populations we modeled are at the southern extent of the species' range (Selong et al. 2001, Wenger et al. 2011). Notice that we modeled this effect with a 1-yr time lag. We expected environmental conditions in the previous year to influence recruitment of age 1 individuals into the current year's population. $\text{temp}_{i,t-1}$ was centered and scaled (i.e., subtract the mean among all years and populations, divide by the standard deviation).

The variable $\text{flow}_{i,t-1}$ is peak stream discharge (maximum 3-day average) estimated using surface flows from the National Land Data Assimilation System (Xia et al. 2012) at the downstream-most point of each population extent. We expected population growth to increase after high flows because of their potential to increase production (Bellmore et al. 2017) and available space (Dunham and Vinyard 1997). $\text{flow}_{i,t-1}$ was centered and scaled on a per-population basis so that it reflected deviations from each population's normal peak discharge.

We included two predictors of density-dependence

$$\phi_{i,t} = \gamma_0 + \gamma_1 \text{nonativ}_{i,t} + \gamma_{2\text{elev}_i} \text{ndvi}_{i,t}$$
$$\boldsymbol{\gamma} \sim \text{Normal}(0, 1) \qquad (6)$$

The normal priors for elements in the vector of regression coefficients γ were selected to be uninformative. Different priors from Eqs. 5 and 6 reflect differences in scale between r and ϕ.

The variable $\text{ndvi}_{i,t}$ is a satellite-derived measure of riparian vegetation condition based on the Normalized Difference Vegetation Index (NDVI; Pettorelli et al. 2011). The variable elev_i is a binary indicator variable that is 1 for populations below 2,000 m elevation and 2 for populations above 2,000 m. This represents two separate effects of $\text{ndvi}_{i,t}$ above and below the ecotone between sagebrush-steppe and montane forests within the Great Basin where riparian communities are dominated by willow–sedge or alpine forests, respectively. We expected a weaker effect of density dependence (i.e., increased carrying capacities) when riparian zones were greener (i.e., higher NDVI) due to the association with greater vegetation cover and primary productivity (Sellers 1985) and the corresponding influence on trout habitat via stream shading, habitat complexity, and terrestrial food subsidies (Wesche et al. 1987, Zoellick 2004, Baxter et al. 2005). We expected this effect to be particularly strong for low elevation sites where there is greater riparian disturbance from cattle grazing (Li et al. 1994, Saunders and Fausch 2012, 2017). We calculated NDVI based on surface reflectance Landsat images (Landsat 5, 7, and 8) using Google Earth Engine (Gorelick et al. 2017). For each year, we identified the peak NDVI value observed during the late growing season (day of year 206–260) and calculated a spatial average with a 25-m buffer of each population's spatial extent. The variable $\text{ndvi}_{i,t}$ was centered and scaled on a per-population basis.

The variable $\text{nonativ}_{i,t}$ is an index of nonnative trout density estimated based on field data obtained from project partners. Nonnatives included rainbow trout (*Oncorhynchus mykiss*), brown trout (*Salmo trutta*), brook trout (*Salvelinus fontinalis*), and hybrids. We expected stronger density dependence (i.e., reduced carrying capacities) as nonnative trout densities increased (Seegrist and Gard 1972, Dunham and Vinyard 1997, Dunham et al. 2002). Nonnative densities were calculated by summing counts among all sites and dividing by the total length of stream reaches sampled. This did not account for imperfect detection or sampling error. Years with missing data were common. In consultation with experienced LCT biologists, we filled in missing data with zeros for streams thought to be free of nonnatives. For other streams, a moving weighted average was used to fill in missing data. The variable $\text{nonativ}_{i,t}$ was scaled (divide by the standard deviation among all years and populations) but not centered, so that other regression coefficients reflected conditions with zero nonnatives.

To accommodate data from historical fish translocations for Lahontan cutthroat, we added the following modification:

$$\tilde{N}_{i,t-1} = N_{i,t-1} + a_{i,t-1}. \tag{7}$$

This included additions to recipient populations ($a_{i,t-1} > 0$) and removals from donor populations ($a_{i,t-1} < 0$). We plugged the supplemented $\tilde{N}_{i,t-1}$ into Eqs. 1 and 4 to provide a mechanism for populations to recover after extirpation from isolated streams, an observed pattern that could not otherwise be represented by our Ricker model. We assumed that translocated individuals survived and reproduced at the same rates as resident fish because we did not have data to support better estimates. Effects of violating this assumption would be minor.

The population time series must be initialized, and we chose the year before the first year with field surveys ($t = 0$) for each population

$$N_{i,0} \sim \text{Poisson}(\lambda_i)$$
$$\lambda_i \sim \text{Gamma}(1 \times 10^{-3}, 1 \times 10^{-3}) \tag{8}$$

The Gamma distribution is the conjugate prior for the Poisson parameter and we chose the Gamma hyperparameters to be minimally informative.

Sampling model.—The focus of the sampling model is to estimate the probability $\upsilon_{i,t,j}$ that an individual from the population would occupy a given sampling location j. This reflects relative habitat suitability at a site compared to available habitat throughout the population extent. This parameter relates population sizes $N_{i,t}$ from the process model to site abundances $n_{i,t,j}$ from the observation model: $E(n_{i,t,j}) = N_{i,t}\upsilon_{i,t,j}$.

We estimated the probability $\upsilon_{i,t,j}$ that an individual would occur at a given site as a binomial process

$$n_{i,t,j} \sim \text{Binomial}(\upsilon_{i,t,j}, N_{i,t}) \tag{9}$$

where $n_{i,t,j}$ is the number of individuals from the total population that occur at site j. We assume with Eq. 9 that individuals could occur at multiple sites surveyed within a population in a year. If we assume that individuals are randomly distributed throughout the spatial extent of each population (i.e., no habitat selection) then a good approximation of the occurrence probability would be $\upsilon_{i,t,j} = \hat{E}_{i,t,j}/E_i$, where $\hat{E}_{i,t,j}$ is the spatial extent of sample site j (e.g., area or length of site) and E_i is the total population extent. For example, if site j represents 5% of the population extent, we would expect about 5% of the population to occur there.

Habitat selection and other processes resulting in non-random distributions of individuals will cause deviations from this expectation. We can account for this by modeling occurrence probabilities $\upsilon_{i,t,j}$ as stochastic. Beta regression (Ferrari and Cribari-Neto 2004) provides a good framework

$$\upsilon_{i,t,j} \sim \text{Beta}(\bar{\upsilon}_{i,t,j}\tau, (1 - \bar{\upsilon}_{i,t,j})\tau)$$
$$\bar{\upsilon}_{i,t,j} = \frac{\hat{E}_{i,t,j}}{E_i} \tag{10}$$

where $\bar{\upsilon}_{i,t,j}$ is the expected occurrence probability at site j (i.e., mean of the Beta distribution) and τ is the precision of the Beta distribution. In practice, the Beta distribution must be truncated to avoid values of one or zero where the density may be infinity. We truncated the Beta distribution between 1×10^{-10} and $1 - 1 \times 10^{-10}$. We used an uninformative uniform prior for sampling precision

$$\tau \sim \text{Uniform}(0, 1 \times 10^4). \tag{11}$$

Sampling precision τ will be low when survey data suggest that site abundances strongly deviate from the expectation of $n_{i,t,j} = N_{i,t}\bar{\upsilon}_{i,t,j}$. This would mean that site densities differ from the overall population density ($n_{i,t,j}/\hat{E}_{i,t,j} \neq N_{i,t}/E_i$). If

individuals were *not* selecting habitat or clustering for other reasons, we would expect the overall population density and all site densities to be equal and for sampling precision τ to be high.

So far, we have not included any survey data in the sampling model. Remember, our data are counts of individuals $y_{i,t,j,m}$ observed during each survey pass m at site j. Assuming no individuals were captured at multiple sites, we also know the total number of individuals observed among all sites sampled in a given year $Y_{i,t} = \sum_{j=1}^{J_{i,t}} \sum_{m=1}^{M_{i,t,j}} y_{i,t,j,m}$. This total count $Y_{i,t}$ for a population in a given year is important because it is the only observed data related directly to total population size

$$Y_{i,t} \sim \text{Binomial}(\varrho_{i,t}, N_{i,t})$$
$$\varrho_{i,t} = 1 - \prod_{j=1}^{J_{i,t}} 1 - \upsilon_{i,t,j}\tilde{P}_{i,t,j} \quad (12)$$

where $\varrho_{i,t}$ is the probability that an individual from population i occupied any surveyed site in year t and was also captured in a survey. $\tilde{P}_{i,t,j}$ is the probability that an individual at site j was detected during one of the survey passes conducted there (see Observation model).

Eq. 12 provides more information about the magnitude of $N_{i,t}$ than Eq. 9, but it relies on the additional assumption that an individual can only be captured at one sampling location in a given year. This information about the magnitude of $N_{i,t}$ is important because the process model only accounts for changes in $N_{i,t}$ from year to year, not its overall magnitude. Notice that Eqs. 9 and 12 have somewhat conflicting assumptions: that individuals could occur at multiple survey sites within a year (Eq. 9), but they could only be captured at one site (Eq. 12). Population sizes $N_{i,t}$ would be overestimated if individuals were frequently captured at multiple sites. Double-counting individuals is unlikely when sample sites cover only a small portion of the population extent, as in our case study.

For Lahontan cutthroat trout, we delineated the total extent E_i of each population based on (1) population delineations in the range-wide status assessment (USFWS, 2009), (2) where the most upstream and downstream LCT were observed, (3) elevation limits estimated by the topographic-thermal niche model of Warren et al. (2014), (4) known barriers to fish movement, and (5) expert opinion from experienced field biologists. Lengths of sampled sites $\hat{E}_{i,t,j}$ were obtained from field notes.

Observation model.—The focus of the observation model is to estimate the probability $p_{i,t,j,m}$ that an individual present during a site survey would be captured. There have been observation models developed for many common survey designs including mark–recapture surveys, repeated point counts, and removal sampling. We will start with a model for repeated point counts for simplicity and consistency with work on N–mixture models (Royle 2004, Dail and Madsen 2010, Zipkin et al. 2014), and we will build toward a removal sampling model customized for Lahontan cutthroat trout.

For repeated point count surveys (i.e., sampling with replacement), observed counts $y_{i,t,j,m}$ for each survey pass m at site j can be modeled as

$$y_{i,t,j,m} \sim \text{Binomial}(p_{i,t,j,m}, n_{i,t,j})$$
$$\text{logit}(p_{i,t,j,m}) = \theta_0 + \theta_1 x_{i,t,j,m} +$$

where $p_{i,t,j,m}$ are pass-specific detection probabilities, and $n_{i,t,j}$ are true site abundances. To account for effects of site conditions on detection probabilities, it is often desirable to include site- or pass-specific covariates $x_{i,t,j,m}$ using logit regression. As written, this model assumes that covariates affect detection probabilities consistently at all sites and populations, but this assumption could be relaxed using random effects.

For Lahontan Cutthroat Trout, electrofishing surveys included either single-pass or multi-pass removal sampling where captured fish were temporarily removed from the stream while additional survey passes were conducted (i.e., sampling *without* replacement). This provides additional information about detectability because we know that fish captured during the third pass were present but not detected during the first and second passes. Block nets were usually (but not always) placed at the upstream and downstream end of stream reaches being sampled. Fish collected during each pass were counted and their lengths recorded. We used counts of age 1+ fish as our response variable. Age 1 + fish were defined as those longer than 60 mm for surveys prior to August and greater than 80 mm after August based on age-length frequencies reported by Neville et al. (2016).

Removal sampling provides two pieces of data: pass-specific counts $y_{i,t,j,m}$ and the total number of fish $Y_{i,t,j}$ captured among all survey passes at a site. Our first data model relates true site abundances $n_{i,t,j}$ to total observed fish

$$Y_{i,t,j} \sim \text{Binomial}(\tilde{P}_{i,t,j}, n_{i,t,j})$$
$$\tilde{P}_{i,t,j} = 1 - \prod_{m=1}^{M_{i,t,j}} 1 - p_{i,t,j,m} \quad (13)$$

where $\tilde{P}_{i,t,j}$ is the probability that a fish occupying site j would be captured in any of the $M_{i,t,j}$ survey passes conducted there and $p_{i,t,j,m}$ is the capture probability for a fish present during the mth electrofishing pass.

Our second data model relates total fish counts $Y_{i,t,j}$ to pass-specific counts

$$\mathbf{y}_{i,t,j,(m)} \sim \text{Multinomial}(\Gamma_{i,t,j,(m)}, Y_{i,t,j})$$
$$\Gamma_{i,t,j,m} = \frac{p_{i,t,j,m}Q_{i,t,j,m}}{\tilde{P}_{i,t,j}}. \quad (14)$$

We used parentheses notation in the indexing for $y_{i,t,j,m}$ and $\Gamma_{i,t,j,m}$ to indicate vectors with an element for each pass m conducted at site j. $\Gamma_{i,t,j,m}$ is the conditional probability that a fish was captured during pass m and not during previous passes, given that it was detected in one of the passes conducted. $Q_{i,t,j,m}$ is the probability of *not* capturing a fish that was present during all previous survey passes

$$Q_{i,t,j,1} = 1$$
$$Q_{i,t,j,m}|_{m>1} = \prod_{\check{m}=1}^{m-1} 1 - p_{i,t,j,\check{m}} \quad (15)$$

In contrast to the assumption of equal capture probabilities among passes underlying many abundance estimators, it has been demonstrated that detection rates for salmonids decline with each subsequent electrofishing pass (Peterson et al. 2004, Rosenberger and Dunham 2005). We specified an exponential model to allow for this

$$p_{i,t,j,m} = p_{i,t,j,1}e^{\delta(m-1)}$$
$$\text{logit}(p_{i,t,j,1}) = \theta_0 + \theta_1\text{drain}_{i,t,j}. \tag{16}$$

We modeled first-pass detection probabilities ($m = 1$) as a function of drainage area $\text{drain}_{i,t,j}$ at sampled sites. We expected detection rates to decline in larger streams. We are not aware of other observation models for removal sampling that include declining detection rates and also share information among sites to bolster inference power, although similar approaches have been used independently (Otis et al. 1978, Mantyniemi et al. 2005, Rivot et al. 2008).

We used uninformative normal priors for parameters in the observation model

$$\theta_0, \theta_1, \delta \sim \text{Normal}(0, 10) \tag{17}$$

We could have used informative priors for θ_0 and δ based on previous empirical estimates (Peterson et al. 2004, Rosenberger and Dunham 2005), but we chose instead to preserve our ability to conduct an unbiased comparison of MPVA parameter estimates to these previous studies. In practice, $p_{i,t,j,m}$ cannot be zero because then $\Gamma_{i,t,j,m}$ may be undefined, so we set a limit where $p_{i,t,j,m} > 0.001$.

Model fitting and evaluation

Our MPVA model was implemented using JAGS software (Plummer 2015) and the R package runjags (Denwood 2013, R Core Team, 2016). The fitted JAGS model (with data and model code) is included as Data S1. We ran 10 chains in parallel on separate processing cores using the "parallel" method of the run.jags() function. A total of 14,401,501 Markov chain Monte Carlo (MCMC) iterations were run for each of 10 chains with a burn-in period of 1,000,000 iterations and a thinning rate of 500. A total of 26,804 MCMC samples were retained from each chain. Convergence was assessed using the Gelman-Rubin statistic (Gelman and Rubin 1992) from the R package coda (Plummer et al. 2006). Gelman-Rubin statistics (also known as potential scale reduction factors) with upper confidence limits less than 1.1 were interpreted as indicating convergence for a parameter (Gelman et al. 2013).

We evaluated model fit graphically by comparing posterior predictions to the observed data: $y_{i,t,j,m}$, $Y_{i,t,j}$, and $Y_{i,t}$. This is a very weak test of the model's ability to estimate population sizes or extinction risks because (1) the model was fit to these data and should predict them well, and (2) posterior predictions are constrained by observed data in other parts of the model (e.g., predicted $\hat{y}_{i,t,j,m}$ is constrained by observed $Y_{i,t,j}$). Poor fit here would indicate a lack of basic error structure to accommodate variation in the observed data.

We evaluated out-of-sample prediction accuracy using both temporal and spatial cross-validations. Forecast accuracy was assessed by withholding the last year of data for each population, refitting the model, and then forecasting population dynamics to the last year of data. Spatial prediction accuracy was assessed by witholding all data from the five populations with the most data, refitting the model, and then predicting population dynamics for each of the five time series. The first year of data from these populations was retained in the model to initialize the time series. For all cross-validations, we compared observed survey data (withheld from model fitting) to model-based predictions of survey results expected at those sites. This is a severe test of model fit because it not only requires accurate estimates of population sizes but also accurate predictions of survey results at specific sites. For this reason, we focused our cross-validation assessment on $Y_{i,t}$ because it aggregates data among sites and is therefore least dependent on site-specific predictions.

We summarized residuals for in-sample model fit and out-of-sample cross-validations by measuring bias (mean of residuals), imprecision (standard deviation of residuals), and inaccuracy (mean of absolute residuals). Residuals of $Y_{i,t}$ and $Y_{i,t,j}$ are not comparable among populations because different numbers of sites may have been sampled (i.e., 1–44 sites) and those sites may differ in size (i.e., 24–200 m) and number of survey passes conducted (i.e., one to six passes). Therefore, we focused on $y_{i,t,j,m}$ for summarizing residuals because they are more comparable among populations and sites, but we still needed to standardize by the length of sample sites to make them comparable. We standardized $y_{i,t,j,m}$ into units of fish captured per 30 m to reflect the most common site length.

Forecasting

A fitted MPVA model can forecast population dynamics and extinction risks by applying process model parameters to future covariate scenarios. There are many ways to construct time series to represent future covariate scenarios, but we chose a simple resampling procedure based on historical conditions. For each forecast year in a population, we randomly selected a year from that population's historical record and used all covariate values from that year for the forecast year. Resampling with replacement was repeated for each forecast year to construct a future covariate time series for a population. Hundreds or thousands of time series may be constructed with parameter values from each MCMC iteration. This approach preserves relationships among covariates (e.g., warmer years tend to have lower stream flows) and randomizes the sequence of environmental conditions from year to year. This procedure assumes that future conditions will be similar to historical conditions.

We created stand-alone R functions to simulate different future covariate scenarios and to forecast population dynamics based on MPVA parameter estimates (i.e., saved MCMC samples). Scenarios could include reintroductions of Lahontan cutthroat trout, changes in nonnative trout densities, and changes in total population extent. Future environmental stochasticity could also be manipulated to represent different frequencies of extreme events (e.g., catastrophes or rare migration events).

We developed a graphical user interface (Data S2) using the R packages shiny (Chang et al. 2017) and leaflet (Cheng

et al. 2017). This provided managers and decision-makers direct access to the model so they could estimate extinction risks for any population and evaluate effects of different environmental and management scenarios. Populations can be explored on an interactive map; results from each population can be easily accessed in graphs and tables (e.g., population forecasts, demographic rates, environmental conditions, raw data); and future scenarios can be manipulated from a menu of buttons and slider bars.

The forecasting results presented here for Lahontan cutthroat trout were based on a 30 year forecast period from 2015 to 2045 (see Appendix S1 for an example). We ran 100 forecast simulations for each of 53,610 MCMC samples (thinned from the full model) for each population. Confidence intervals for extinction risks represented variation among the 100 simulations. See Data S2 for code and data.

Results

We detected covariate effects on demographic rates and detection probabilities that were consistent with expectations (Fig. 2, Table 2). Cold streams and high flushing flows in the previous year were positively related to recruitment into the current year's population. Densities of nonnative trout were negatively related to carrying capacities of Lahontan cutthroat trout populations (i.e., caused $\phi_{i,t}$ to be more negative). Greener riparian vegetation had a weak positive relationship with carrying capacities in low elevation sagebrush steppe, but no effect in higher elevation populations with forested catchments. The effects of water temperature and nonnative trout were statistically significant at the 95% confidence level, but effects of high flow and riparian vegetation were not (Table 2).

As an example, we will present results from a population in a 7.3 km segment of Abel Creek in the Santa Rosa Range of northern Nevada (see Appendix S1). This stream had a mean August water temperature of 13.2°C, which was about average among streams that we assessed. The most recent density of nonnative trout at Abel Creek was 139 trout/km, higher than most streams. Assuming future conditions will be similar to historical conditions for this population, MPVA estimated its probability of extinction by the year 2045 to be
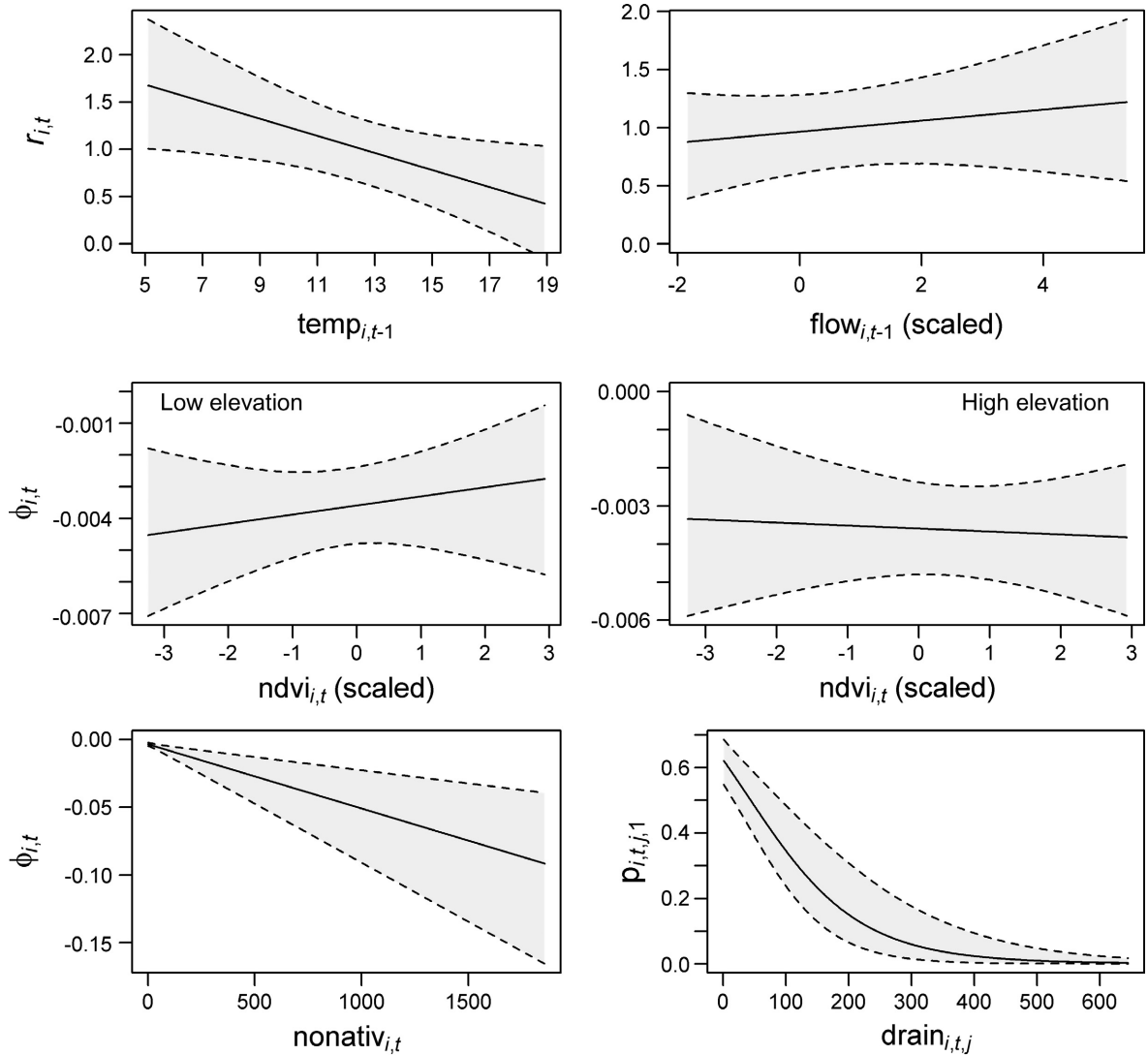

FIG. 2.   Effects of covariates on intrinsic population growth rates $r_{i,t}$, density-dependence $\phi_{i,t}$, and first-pass detection rates $p_{i,t,j,1}$.

TABLE 2. Means and quantiles of posterior densities for MPVA parameters.

Parameter	Mean	2.5%	5%	25%	50%	75%	95%	97.5%
β_0	0.964	0.604	0.672	0.859	0.971	1.076	1.231	1.281
β_1	−0.181	−0.343	−0.316	−0.236	−0.181	−0.125	−0.047	−0.021
β_2	0.048	−0.076	−0.057	0.003	0.046	0.091	0.157	0.18
γ_0	−0.0036	−0.0048	−0.0046	−0.004	−0.0036	−0.0032	−0.0026	−0.0024
γ_1	−0.0119	−0.0219	−0.0198	−0.0145	−0.0114	−0.0088	−0.0057	−0.0049
γ_{2low}	0.00029	−0.00057	−4e−04	6e−05	0.00032	0.00055	0.00087	0.00097
γ_{2high}	−8e−05	−0.00074	−0.00062	−0.00029	−7e−05	0.00014	0.00044	0.00054
μ_σ	1.084	0.914	0.943	1.028	1.085	1.141	1.224	1.252
σ_σ	0.302	0.137	0.156	0.23	0.291	0.361	0.485	0.533
τ	307	279	283	297	307	317	332	336
θ_0	−0.219	−0.628	−0.566	−0.373	−0.226	−0.073	0.158	0.232
θ_1	−2.25	−2.99	−2.88	−2.52	−2.27	−1.99	−1.56	−1.4
δ	−0.518	−0.685	−0.661	−0.582	−0.522	−0.457	−0.359	−0.329

17.6% (16.8–18.5%). That assumes a constant density of 139 nonnative trout per kilometer. Increasing the density of non-natives back to the highest historical level from this stream (661 per km) raised the extinction risk to 22% (19.7–25.2%). When we simulated the removal of nonnatives from Abel Creek, extinction risk was reduced to 12.9% (13.7–14.6%).

Differences in extinction risks among populations were associated with several factors (Figs. 3 and 4). Populations with the most environmental stochasticity always had very high extinction risks, and populations with the lowest environmental stochasticity always had very low extinction probabilities. Most, however, had moderate environmental stochasticity and a range of extinction risks. The relationship of extinction risk with other parameters was less pronounced, but a few trends were observed (Fig. 3). Populations occupying more than 15 stream km usually had extinction risks <50%. Almost all populations in streams with average summer water temperatures below 11°C had extinction risks less than 50%. The median extinction risk for streams without nonnative trout was 27% (quartiles = 14–42%), whereas the median extinction risk was 47% (23–86%) for streams with nonnative trout. Populations with high extinction risks were almost always in streams with average August water temperatures above 11°C or with less than 15 km of available habitat.

MPVA estimated detection rates for first survey passes in average sized streams (63 km^2 drainage) to be 45%, and to decline to 27% in the second pass and 16% in the third pass (Fig. 5). These results are consistent with previous experimental evaluations of detection rates for salmonids with backpack electrofishing in streams (Peterson et al. 2004, Rosenberger and Dunham 2005). Our results also indicated that detection rates were significantly reduced in larger streams (Fig. 2).

Posterior predictions matched very well to the observed data that were used for model fitting (Fig. 6, Table 3). One exception was the error structure in our observation model, which did not quite accommodate all of the variation in the data (i.e., a few credible intervals do not overlap the 1:1 line in Fig. 6). We explored the addition of an error term in the observation model (i.e., beta regression for $p_{i,t,j,1}$), but this led to identifiability issues among observation error, sampling precision τ, and the intercept for detection θ_0, and so was not used.

As expected, cross-validation results showed fits that were much worse than the fit to model data (Fig. 7, Table 3). Spatial and temporal predictions were relatively unbiased,

but they were imprecise. Spatial cross-validations were most imprecise because these predictions relied almost entirely on covariates, whereas temporal cross-validations were constrained by fish counts from previous years. Note that spatial cross-validation used the first year of data to initialize the time-series, but in reality MPVA predictions at new locations will usually not have these data. If new locations are being considered for reintroductions, the expected number of animals to be introduced can be used to initialize an MPVA time series, otherwise an educated guess would be required and this may affect prediction accuracy.

All root node parameters in the model converged. Population-specific estimates of environmental stochasticity did not converge for 28 populations due to insufficient data. We used random draws from Half-Cauchy(μ_σ, σ_σ) to represent environmental stochasticity in these populations, just as we would for populations with no survey data.

DISCUSSION

We consider MPVA to be an adaptive management tool (sensu Walters 1986). It provides explicit estimates of uncertainty to support informed decision making and it requires periodic updates with new data and model structures to keep pace with improving ecological knowledge and changing management needs. A fitted hierarchical MPVA can be used in a variety of ways to meet conservation objectives. It can help target data collection towards populations where uncertainty is greatest, as more data from those populations will reduce uncertainty when the model is updated. A fitted model can use simulated covariate scenarios to evaluate potential risk reduction due to management actions in real populations (e.g., reintroductions, nonnative removals). It can identify habitat characteristics related to population declines and it can assess the risk posed by environmental stochasticity when populations are small.

Model extensions

We focused on an observation model for removal sampling, but various other observation models could be developed for hierarchical MPVA to accommodate other survey designs such as point counts, distance sampling, multi-observer surveys, or mark–recapture studies (Royle and
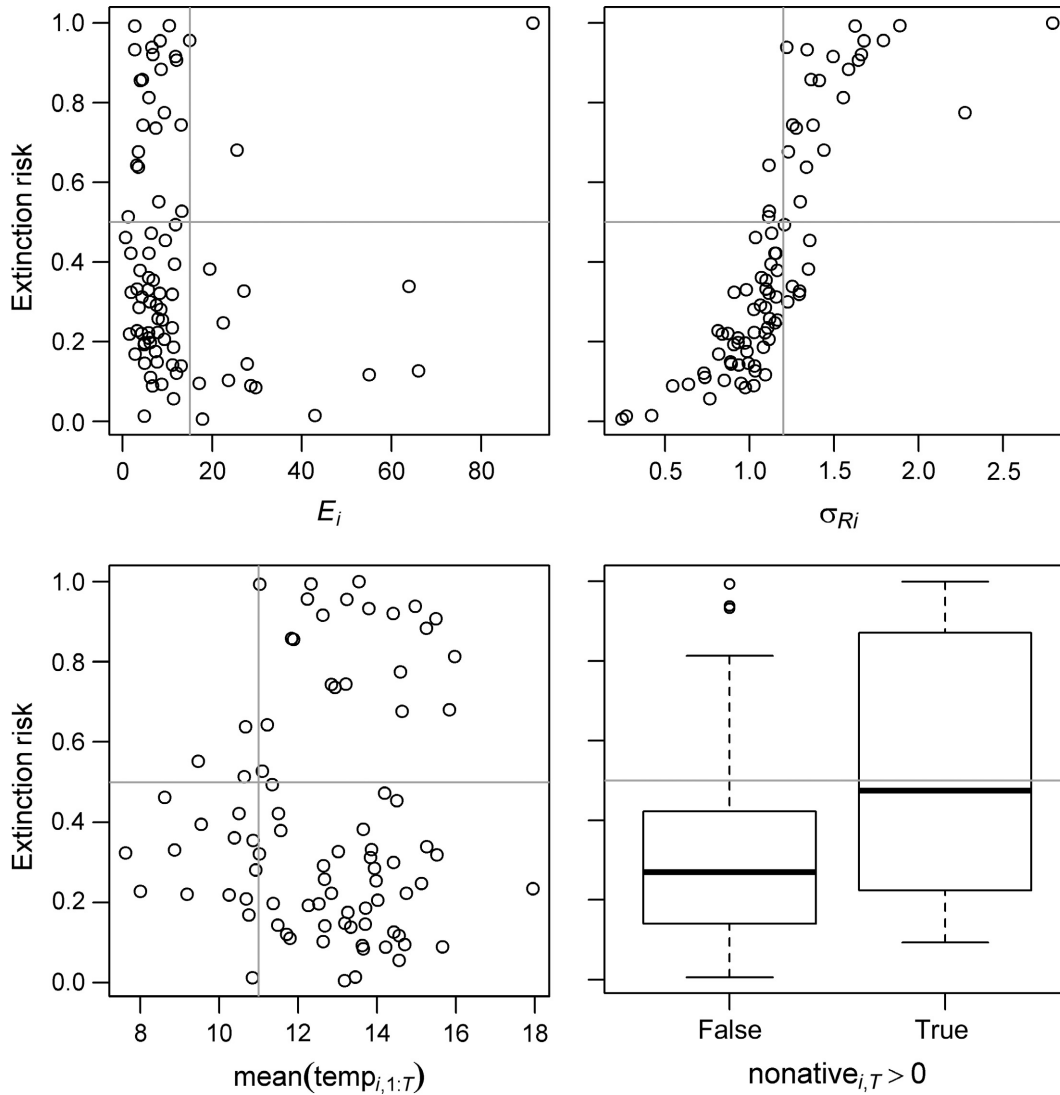
Fig. 3. Extinction risks across all populations in response to population extent (E_i), environmental stochasticity (σ_{R_i}), average stream temperature (mean($temp_{i,1:T}$)), and the most recent observed density of nonnative trout ($nonativ_{i,T}$). Vertical lines are thresholds beyond which extinction risks tend to be less than 50% ($E_i > 15km$; $\sigma_{R_i} < 1.2$; mean($temp_i$) < 11°C). Points represent individual populations. In the boxplot, mid-lines represent median values, box edges represent interquartile ranges, and whiskers extend to the most extreme data points not exceeding 1.5 times the interquartile range.

Dorazio 2008). It may also be possible to apply different observation models to subsets of data within an MPVA when historical data sets were obtained using multiple survey designs (Shaub and Abadi 2011).

In the sampling model, it would be ideal to include site-level covariates that influence occurrence probabilities. This would essentially create population- and year-specific species distribution models nested within the MPVA model. Additional work is needed to extend our MPVA covariate structure to account for habitat in un-sampled portions of a population's extent. A Dirichlet-Multinomial sampling model may be more appropriate when individuals cannot move among sites.

Within the process model, stage-structured models (Leslie 1945, Zipkin et al. 2014) or meta-population models (Hanski and Gilpin 1997) are obvious extensions that could potentially be incorporated when appropriate data are available. The Ricker model could also be replaced with a

Beverton-Holt model (Beverton and Holt 1957) or logistic growth model (Verhulst 1838). Another useful addition may be region-based random intercepts or spatial block covariance to constrain nearby populations to be similar to one another or to covary through time (Cressie and Wikle 2011).

Challenges

Although MPVA benefits from sharing information among populations, it still requires a substantial amount of data. The minimum data requirements depend on the characteristics of the biological system (e.g., degree of environmental stochasticity, spatial extent of populations, longevity of organisms), the level of model complexity (e.g., covariates, variance structure, type of observation model), and strength of priors. With informative priors, an MPVA model can be fit with few data, but the effectiveness of such an exercise will depend on the suitability of prior estimates.
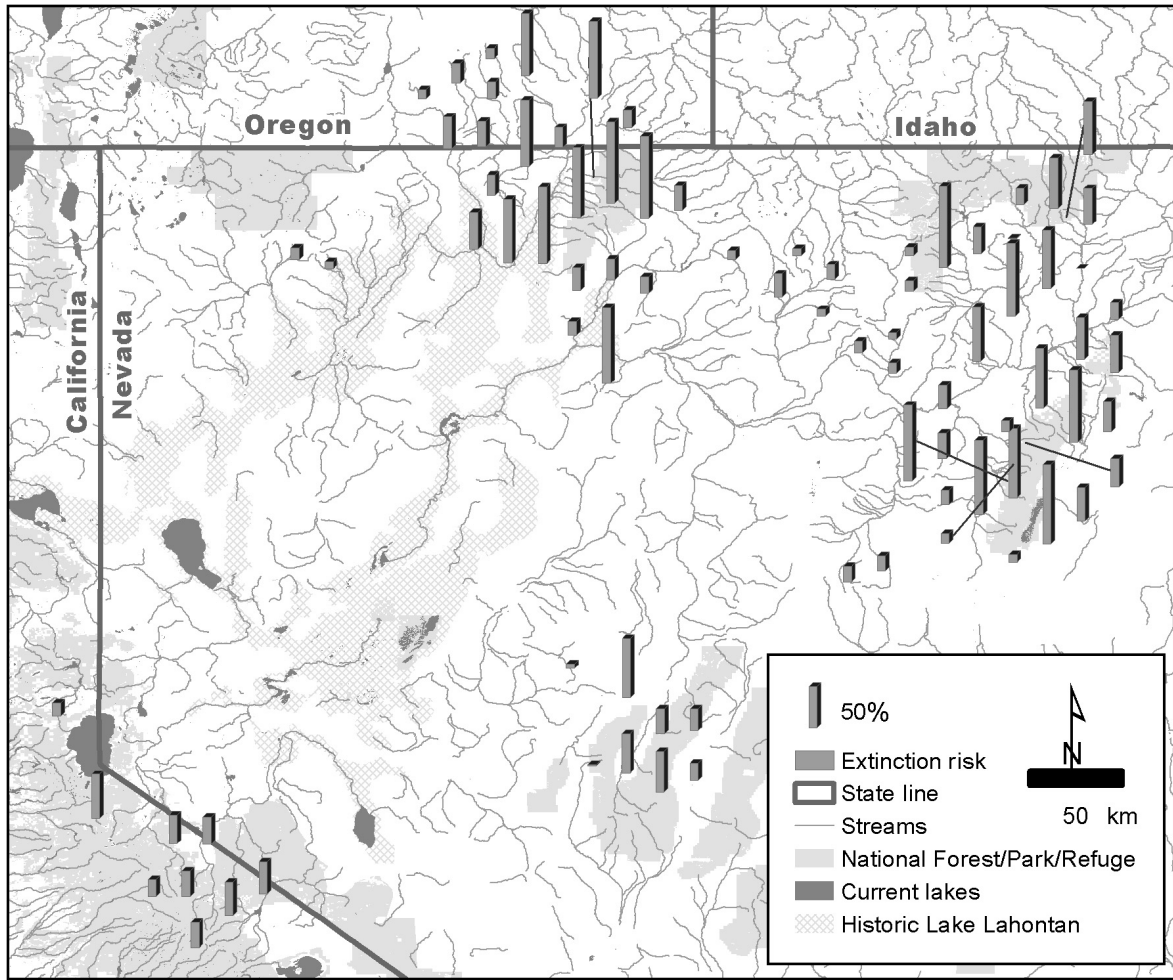
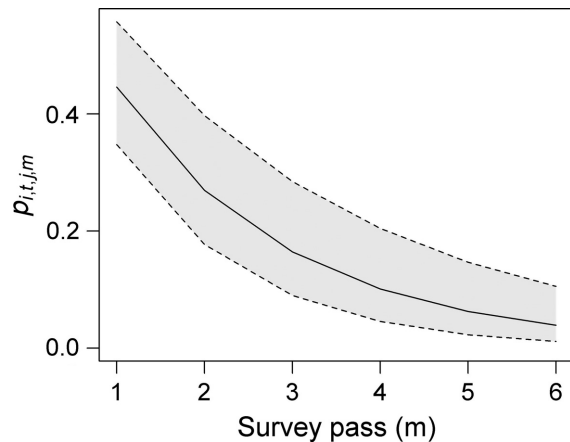Fig. 4. Map of extinction risks for current Lahontan cutthroat populations.

Fig. 5. Detection rates $p_{i,t,j,m}$ expected during each electrofishing pass in an average-sized stream (i.e., 62-km² drainage).

It is difficult to include field-based habitat measurements in MPVA because covariates must be measured consistently among all populations and years. Missing data in the covariate time series (e.g., years when field surveys were not conducted) must be filled in and this introduces measurement error. In some cases, noisy field measurements are adequate because the signal is strong, as was the case with nonnative trout in our example. In most cases, MPVA will rely heavily on GIS and remotely sensed covariates. Fortunately, appropriate data are widely available (Dauwalter et al. 2017, Gorelick et al. 2017).

Assessing model fit for hierarchical MPVA is a challenge. A fair test would be to compare predicted population sizes to observed population sizes or extinction outcomes, but it is usually not possible to measure these response variables directly (a problem for all PVAs). Posterior predictive checks are often used to assess Bayesian model fit. These compare model predictions to the observed data that were used to fit the model. In our case, that included $y_{i,t,j,m}$, $Y_{i,t,j}$, and $Y_{i,t}$. For MPVA, this would usually indicate excellent fit to data in the model, but it is a biased assessment of forecast accuracy or spatial predictions, the two primary uses of MPVA. Spatial and temporal cross-validations seem ideal for this, but they provide pessimistic estimates of MPVA model fit because they require the model to not only forecast population sizes but to also accurately predict *survey data* at sample sites within those populations. We focused on $Y_{i,t}$ for cross-validation because it was less dependent on site-specific or pass-specific predictions (i.e., it aggregated data among sites).
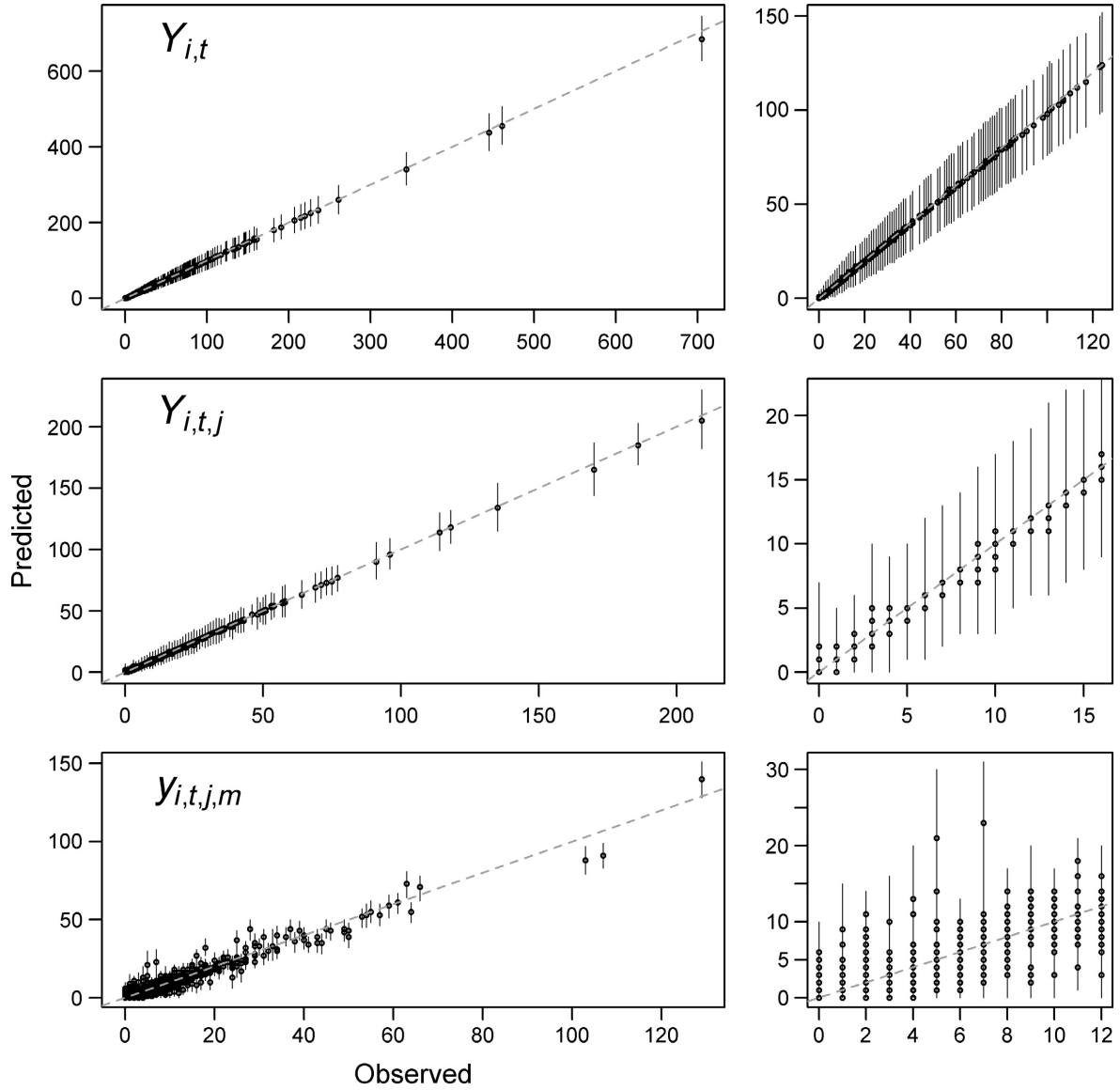
F_{IG}. 6. Observed vs. predicted plots for $Y_{i,t}$, $Y_{i,t,j}$, and $y_{i,t,j,m}$ to assess fit of in-sample posterior predictions showing 95% credible intervals. Panels to the right are zoomed in to the region with 95% of observed data.

T_{ABLE} 3. Summaries of residuals for in-sample posterior predictions and out-of-sample cross validations for $y_{i,t,j,m}$.

Prediction	Bias	Imprecision	Inaccuracy
In-Sample	0	1.4	0.8
Temporal	0.8	7.3	3.0
Spatial	−0.3	14.8	3.4

However, this was still particularly challenging when only a few sites (or a single site) were surveyed or when individuals had clumped spatial distributions within population extents.

We urge users of MPVA to explore the assumptions and behavior of fitted MPVA models using covariate simulations and sensitivity analyses. This is best done on a population-by-population basis because changes in covariates and model parameters may affect extinction risks very differently among populations. For example in our LCT model, a population in a warm stream would be more sensitive to increasing temperatures than a population in a cold stream. Populations restricted to small stream segments may be more sensitive to increases in environmental stochasticity. We recommend graphical user interfaces for fitted MPVA models so that users can explore the sensitivity of individual populations to changes in covariates and model parameters. This allows stakeholders to better understand the strengths and weaknesses of the model overall, and to better interpret results for specific populations where decisions are being made.

Conclusion

Hierarchical multi-population viability analysis (MPVA) provides data-driven estimates of extinction risks by

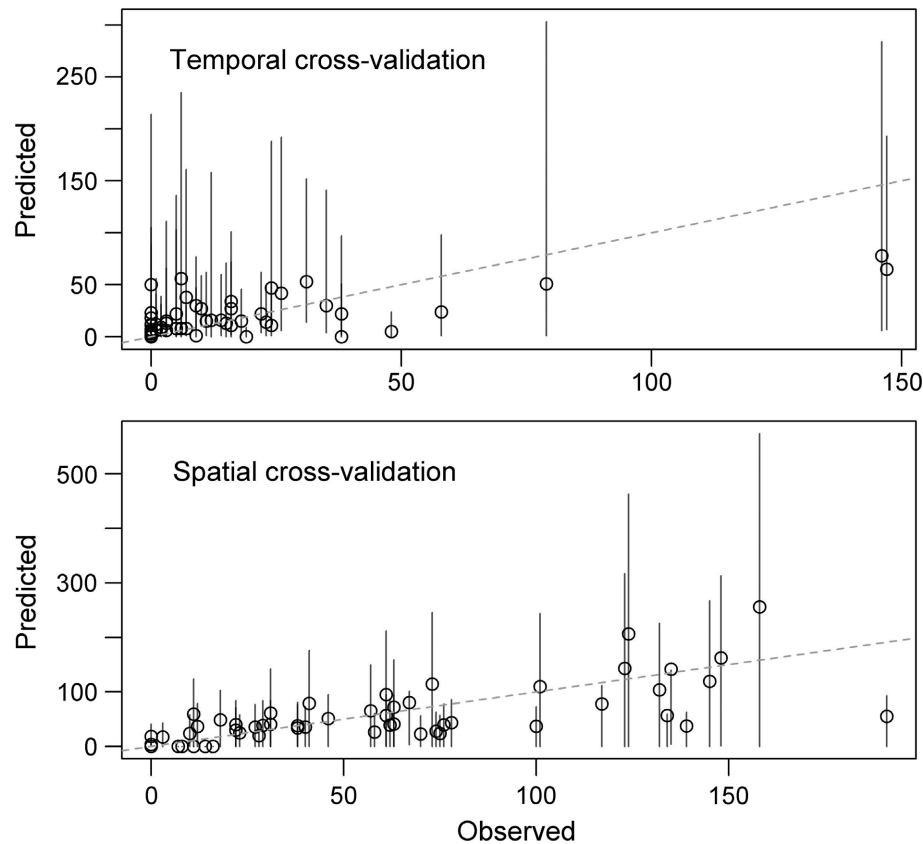
FIG. 7. Spatial and temporal cross-validation results for $Y_{i,t}$ showing 90% credible intervals for predictions.

connecting field observations to theoretical population models. It harnesses the statistical power of sparse datasets by sharing information among multiple populations. With creative user interfaces, we can put these sophisticated models directly into the hands of managers and decision makers. These tools can serve as a focal point for organizing people and information, assessing uncertainty, and making collaborative, well-informed decisions. At its best, hierarchical multi-population viability analysis can be a process that brings together disparate datasets and the biologists who collected them; it can help to formalize prevailing hypotheses and test them against data; and it can provide an objective basis for evaluating risks and prioritizing investments.

LITERATURE CITED

Akcakaya, H. R., and M. G. Raphael. 1998. Assessing human impact despite uncertainty: viability of the northern spotted owl metapopulation in the northwestern USA. Biodiversity and Conservation 7:875–894.

Baxter, C. V., K. D. Fausch, and W. C. Saunders. 2005. Tangled webs: reciprocal flows of invertebrate prey link streams and riparian zones. Freshwater Biology 50:201–220.

Beissinger, S. R., and D. R. McCullough. 2002. Population viability analysis. The University of Chicago Press, Chicago, Illinois, USA.

Bellmore, J. R., J. R. Benjamin, M. Newsom, J. A. Bountry, and D. Dombroski. 2017. Incorporating food web dynamics into ecological restoration: a modeling approach for river ecosystems. Ecological Applications 27:814–832.

Berliner, L. M. 1996. Hierarchical bayesian time series models. Pages 15–22 in K. M. Hanson and R. N. Silver, editors. Maximum entropy and Bayesian methods. Kluwer Academics, Dordrecht, The Netherlands.

Beverton, R. J. H., and S. J. Holt. 1957. On the dynamics of exploited fish populations. Ministry of Agriculture, Fisheries and Food, London, UK.

Boyce, M. S. 1992. Population viability analysis. Annual Review of Ecology and Systematics 23:481–506.

Boyce, M. S. 1994. Population viability analysis exemplified by models for the nothern spotted owl. Pages 3–18 in D. J. Fletcher and B. F. J. Manly, editors. Statistics in ecology and environmental monitoring. University of Otago Press, Dunedin, New Zealand.

Carlin, B. P., N. G. Polson, and D. S. Stoffer. 1992. A monte carlo approach to nonnormal and nonlinear state-space modeling. Journal of the American Statistical Association 87:493–500.

Caughley, G. 1994. Directions in conservation biology. Journal of Animal Ecology 63:215–244.

Chang, W., J. Cheng, J. Allaire, Y. Xie, and J. McPherson. 2017. shiny: Web Application Framework for R. R package version 1.0.1. https://cran.r-project.org/package=shiny

Cheng, J., B. Karambelkar, and Y. Xie. 2017. leaflet: Create Interactive Web Maps with the JavaScript 'Leaflet' Library. R package version 1.1.0. https://cran.r-project.org/package=leaflet

Clark, J. S. 2007. Models for ecological data, an introduction. Princeton University Press, Princeton, New Jersey, USA.

Clark, J. S., and O. N. Bjornstad. 2004. Population time series: process variability, observation errors, missing values, lags, and hidden states. Ecology 85:3140–3150.

Cressie, N., and C. K. Wikle. 2011. Statistics for spatio-temporal data. John Wiley and Sons Inc, Hoboken, New Jersey, USA.

Dail, D., and L. Madsen. 2010. Models for estimating abundance from repeated counts of an open metapopulation. Biometrics 67:577–587.

Dauwalter, D. C., K. A. Fesenmyer, R. Bjork, D. R. Leasure, and S. J. Wenger. 2017. Satellite and airborne remote sensing applications to freshwater fisheries. Fisheries 42:526–537.

Denwood, M. J.. 2013. runjags: An r package providing interface utilities, parallel computing methods and additional distributions for mcmc models in jags. Journal of Statistical Software 1:0–7.

Doak, D. F. 1989. Spotted owls and old growth logging in the pacific northwest USA. Conservation Biology 3:389–396.

Dunham, J. B., and G. L. Vinyard. 1997. Habitat fragmentation and extinction risk of lahontan cutthroat trout. North American Journal of Fisheries Management 17:1126–1133.

Dunham, J. B., S. B. Adams, R. E. Schroeter, and D. C. Novinger. 2002. Alien invasions in aquatic ecosystems: toward an understanding of brook trout invasions and potential impacts on inland cutthroat trout in western north America. Reviews in Fish Biology and Fisheries 12:373–391.

Ferrari, S. L. P., and F. Cribari-Neto. 2004. Beta regression for modelling rates and proportions. Journal of Applied Statistics 31:799–815.

Gelman, A. 2006. Prior distributions for variance parameters in hierarchical models (comment on article by browne and draper). Bayesian Analysis 1:515–534.

Gelman, A., and D. B. Rubin. 1992. Inference from iterative simulation using multiple sequences. Statistical Science 7:457–511.

Gelman, A., J. B. Carlin, H. S. Stern, D. B. Dunson, A. Vehtari, and D. B. Rubin. 2013. Bayesian data analysis. Third edition. CRC Press, Boca Raton, Florida, USA.

Gorelick, N., M. Hancher, M. Dixon, S. Ilyushchenko, D. Thau, and R. Moore. 2017. Google earth engine: Planetary-scale geospatial analysis for everyone. Remote Sensing of Environment 202:18–27.

Gotelli, N. J. 2008. A primer of ecology. Fourth edition. Sinauer Associates Inc, Sunderland, Massachusetts, USA.

Hanski, I. A., and M. E. Gilpin. 1997. Metapopulation biology: Ecology, genetics, and evolution. Academic Press, San Diego, California, USA.

Hobbs, N. T., and M. B. Hooten. 2015. Bayesian models: A statistical primer for ecologists. First Edition. Princeton University Press, Princeton, New Jersey, USA.

Isaak, D., et al. 2017. The norwest summer stream temperature model and scenarios for the western U.S.: A crowd-sourced database and new geospatial tools foster a user community and predict broad climate warming of rivers and streams. Water Resources Research 53:9181–9205.

Kanno, Y., B. H. Letcher, N. P. Hitt, D. A. Boughton, J. E. B. Wofford, and E. Zipkin. 2015. Seasonal weather patterns drive population vital rates and persistence in a stream fish. Global Change Biology 21:1856–1870.

Lande, R. 1988. Demographic models of the northern spotted owl (strix occidentalis caurina). Oecologia 75:601–607.

Leslie, P. H. 1945. On the use of matrices in certain population mathematics. Biometrika 35:183–212.

Li, H., G. A. Lamberti, T. N. Pearsons, C. K. Tait, J. L. Li, and J. C. Buckhouse. 1994. Cumulative effects of riparian disturbances along high desert trout streams of the john day basin, oregon. Transactions of the American Fisheries Society 123:627–640.

MacKenzie, D. I., J. D. Nichols, J. A. Royle, K. H. Pollock, L. L. Bailey, and J. E. Hines. 2006. Occupancy estimation and modeling. Elsevier, Amsterdam, The Netherlands.

Mantyniemi, S., A. Romakkaniemi, and E. Arjas. 2005. Bayesian removal estimation of a population size under unequal catchability. Canadian Journal of Fisheries and Aquatic Sciences 62:291–300.

May, R. M. 1973. Stability and complexity in model ecosystems. Princeton University Press, Princeton, New Jersey, USA.

Morris, W. F., and D. F. Doak. 2002. Quantitative conservation biology: Theory and practice of population viability analysis. Sinauer Associates, Inc., Sunderland, Massachusetts, USA.

Neville, H., D. Dauwalter, and M. Peacock. 2016. Monitoring demographic and genetic responses of a threatened inland trout to habitat reconnection. Transactions of the American Fisheries Society 145:610–626.

Otis, D. L., K. P. Burnham, G. C. White, and D. R. Anderson. 1978. Statistical inference from capture data on closed animal populations. Wildlife Monographs 62:3–135.

Peacock, M. M., and N. A. Dochtermann. 2012. Evolutionary potential but not extinction risk of lahontan cutthroat trout (oncorhynchus clarkii henshawi) is associated with stream characterisitics. Canadian Journal of Fisheries and Aquatic Sciences 69:615–626.

Peterson, J. T., R. F. Thurow, and J. W. Guzevich. 2004. An evaluation of multipass electrofishing for estimating the abundance of stream-dwelling salmonids. Transactions of the American Fisheries Society 133:462–475.

Pettorelli, N., S. Ryan, T. Mueller, N. Bunnefeld, B. Jedrzejewska, M. Lima, and K. Kausrad. 2011. The normalized difference vegetation index (NDVI): unforseen sucessses in animal ecology. Climate Research 46:15–27.

Plummer, M. 2015. JAGS Version 4.0.0 user manual. http://mcmc-jags.sourceforge.net/

Plummer, M., N. Best, K. Cowles, and K. Vines. 2006. Coda: Convergence diagnosis and output analysis for mcmc. R News 6:7–11.

R Core Team. 2016. R: A language and environment for statistical computing. R Foundation for Statistical Computing, Vienna, Austria.

Ricker, W. E. 1954. Stock and recruitment. Journal of the Fisheries Research Board of Canada 11:559–623.

Rivot, E., E. Prevost, A. Cuzol, J.-L. Bagliniere, and E. Parent. 2008. Hierarchical Bayesian modelling with habitat and time covariates for estimating Riverine fish population size by successive removal method. Canadian Journal of Fisheries and Aquatic Sciences 65:117–133.

Rosenberger, A. E., and J. B. Dunham. 2005. Validation of abundance estimates from mark–recapture and removal techniques for rainbow trout captured by electrofishing in small streams. North American Journal of Fisheries Management 25:1395–1410.

Royle, J. A. 2004. N-mixture models for estimating population size from spatially replicated counts. Biometrics 60:8–115.

Royle, J. A., and R. M. Dorazio. 2008. Hierarchical modeling and inference in ecology. Academic Press, London, UK.

Saunders, W. C., and K. D. Fausch. 2012. Grazing management influences the subsidy of terrestrial prey to trout in central rocky mountain streams. Freshwater Biology 57:1512–1529.

Saunders, W. C., and K. D. Fausch. 2017. Improved grazing management increases terrestrial invertebrate inputs that feed trout in Wyoming rangeland streams. Transactions of the American Fisheries Society 136:1216–1230.

Seegrist, D. W., and R. Gard. 1972. Effects of floods on trout in Sagehen creek, California. Transactions of the American Fisheries Society 101:478–482.

Sellers, P. J. 1985. Canopy reflectance, photosynthesis and transpiration. International Journal of Remote Sensing 6:1335–1372.

Selong, J. H., T. E. McMahon, A. V. Zale, and F. Barrows. 2001. Effect of temperature on growth and survival of bull trout, with application of an improved method for determining thermal

tolerances in fishes. Transactions of the American Fisheries Society 130:1026–1037.

Shaffer, M. L. 1978. Determining minimum viable population sizes: A case study of the grizzly bear (Ursus arctos L.). Ph.D. thesis, Duke University, Durham, North California.

Shaffer, M. L. 1981. Minimum population sizes for species conservation. BioScience 1:131–134.

Shaffer, M. L. 1983. Determining minimum viable population sizes for the grizzly bear. Pages 133–139 in E. Charles Meslow, editor. Bears: Their biology and management, Vol. 5, A selection of papers from the fifth international conference on bear research and management. International Association for Bear Research and Management, Madison, Wisconsin, USA.

Shaub, M., and F. Abadi. 2011. Integrated population models: a novel analysis framework for deeper insights into population dynamics. Journal of Ornithology 152:227–237.

Staples, D. F., M. L. Taper, and B. Dennis. 2004. Estimating population trend and process variation for PVA in the presence of sampling error. Ecology 85:923–929.

USFWS. 2009. Lahontan cutthroat trout (oncorhynchus clarkii henshawi) 5-year review: summary and evaluation. Technical report, U.S. Fish and Wildlife Service, Reno, Nevada, USA.

Verhulst, P. F. 1838. Notice sur la loi que la population poursuit dans son accroissement. Correspondance Mathé-matique et Physique 10:113–121.

Walters, C. 1986. Adaptive management of renewable resources. Macmillan Publishing Company, New York, New York, USA.

Warren, D. R., J. B. Dunham, and D. Hockman-Wert. 2014. Geographic variability in elevation and topographic constraints on the distribution of native and nonnative trout in the great basin. Transactions of the American Fisheries Society 143:205–218.

Wenger, S. J., et al. 2011. Flow regime, temperature, and biotic interactions drive differential declines of trout species under climate change. Proceedings of the National Academy of Sciences USA 108:14175–14180.

Wenger, S. J., D. R. Leasure, D. C. Dauwalter, M. Peacock, J. Dunham, H. Neville, and N. Chelgren. 2017. Viability analysis of multiple populations. Biological Conservation, 216:69–77.

Wesche, T. A., C. M. Goertler, and C. B. Frye. 1987. Contribution of riparian vegetation to trout cover in small streams. North American Journal of Fisheries Management 7:151–153.

Xia, Y., et al. 2012. Continental-scale water and energy flux analysis and validation for the North American LandData Assimilation System project phase 2 (NLDAS-2): 1. Intercomparison and application of model products. Journal of Geophysical Research 117:D03109. https://doi.org/10.1029/2011JD016048

Zipkin, E. F., J. R. Thorson, K. See, H. J. Lynch, E. H. C. Grant, Y. Kanno, R. B. Chandler, B. H. Letcher, and J. A. Royle. 2014. Modeling structured population dynamics using data from unmarked individuals. Ecology 95:22–29.

Zoellick, B. W. 2004. Density and biomass of redband trout relative to stream shading and temperature in southwestern idaho. Western North American Naturalist 64:18–26.

Supporting Information

Additional supporting information may be found in the online version of this article at http://onlinelibrary.wiley.com/doi/10.1002/ecy.2538/suppinfo